Measurement issues of organic solar cell

Gang Li[1], Vishal Shrotriya[1], Jinsong Huang [2] and Yang Yang[2]
1. Solarmer Energy Inc, El Monte, CA 91731
2. Dept. of MSE, UCLA, Los Angeles, CA 90095

ABSTRACT

Organic solar cells (OSCs) have been extensively studied and significant improvements have been demonstrated in recent years. Along with the excitement in technology development, the accurate measurement of OSCs has become critical for the healthy development of this promising technology. The limited absorption and spectral response of organic based solar cells could lead to significant derivation in solar cell measurement. In this paper, we will discuss several issues in the measurement of organic solar cells, including spectral mismatch factor, elimination of the mismatch by proper selection of reference cell, external quantum efficiency testing, device area issue etc. Results on both polymer based bulk hetero-junction solar cell and small molecule based solar cell will be presented.

Key words: Organic Solar Cell, Organic Photovoltaics, Measurement

1. INTRODUCTION

Organic photovoltaic devices (both polymer and small molecule based) attracted much attention in the last several years and have been advanced significantly [1-6] with NREL certified efficiency of 5.4% in polymer based bulk heterojucntion (BHJ) system. The most common donor polymers that have been used in the past are poly[2-methoxy-5-(3,7-dimethyloctyloxy)-1,4-phenylene vinylene] (MDMO-PPV)[7-9], regioregular poly(3-hexylthiophene) (RR-P3HT)[10-15], and poly[2-methoxy-5-(2'-ethyl-hexyoxy)-1,4-phenylene vinylene] (MEH-PPV)[16,17]. The most common candidate for the acceptor material is [6,6]-phenyl C_{61}-butyric acid methyl ester (PCBM)[18]. Small molecules such as copper pthalocyanine (CuPc)[19-21], zinc pthalocyanine (ZnPc)[22,23], tetracene[24], and pentacene[25] have been used as donors combined with buckminsterfullerene (C_{60}) molecules in a bilayer heterojunction or coevaporated to incorporate BHJ concept to improve the performance. With the efficiencies of organic solar cells are now fast approaching the levels where they could be put into commercial applications, The society also reach consensus that it is critical to consistently measure the efficiency values throughout the society for the healthy development of the technology. Standard test method [26-28] has been established with the world wide effort on inorganic solar cell development. In 1980 the Cell Performance Laboratory was established by DOE at NREL to provide the U.S. terrestrial PV community with standardized efficiency measurement and reference cell calibrations.

In the early 1980's similar laboratories were being set up in Germany, Japan and elsewhere. In the 1980's U.S. and international standards were developed and adopted by the national PV calibration laboratories around the world.[25,26] As a early stage technology, it takes many years for organic solar cells society to adopt these internationally accepted norms at the research level, partially due to lack of awareness of these norms, limited resources, and/or relatively low efficiency. Some efforts in the past have sought to motivate the organic solar cell community toward adopting standards for accurately measuring efficiency.[29.30] In this paper, we present a simple method to accurately determine the efficiency of organic solar cells. We first explore the spectral mismatch factors in different kinds of test cell / reference cell combinations under the standard reference spectrum and show the importance of this parameter in organic solar cell research. We also demonstrate the importance of choosing a suitable reference cell for light-source intensity calibration. The spectral responsivity measurements are performed on various types of test cells, and the effect of light-bias intensity on external quantum efficiency of organic solar cells is discussed. The device area is also an important error source if not measured carefully, especially in small device area (<<1cm^2). Examples on possible source of error are discussed.

2. ORGANIC SOLAR CELL MEASUREMENT

The performance of PV cells is commonly rated in terms of their efficiency with respect to standard reporting conditions (SRC) defined by temperature, spectral irradiance, and total irradiance.[28] The SRC for rating the performance of terrestrial PV cells are the following: 1000 Wm^{-2} irradiance, AM 1.5 global reference spectrum, and 25ºC cell temperature.[31-35] The power conversion efficiency of a PV cell is given as:

*gangl@solarmer.com

Organic Photovoltaics IX, edited by Zakya H. Kafafi, Paul A. Lane,
Proc. of SPIE Vol. 7052, 70520E, (2008) · 0277-786X/08/$18 · doi: 10.1117/12.799607

$$\eta = \frac{P_{\max}}{E_{\text{tot}} A} 100, \tag{1}$$

where $P_{\max}$ is the measured peak power of the cell, A is the device area, and E_{tot} is the total incident irradiance. For Eq. 1 to give a unique efficiency E_{tot} must be with respect to a reference spectral irradiance. The irradiance, E_{tot}, incident on the PV cell is typically measured with a reference cell. For *I-V* measurements with respect to a reference spectrum, there is a spectral error in the measured short-circuit current (I_{SC}) of the PV cell because of the following two reasons: (i) the spectral irradiance of the light source does not match the reference spectrum, which is computer generated, and (ii) the spectral responses of reference detector and test cell are different. This error can be derived based upon the assumption that the photocurrent is the integral of the product of cell responsivity and incident spectral irradiance. This error can be expressed as spectral mismatch correction factor (M):

$$M = \frac{\int_{\lambda_1}^{\lambda_2} E_{\text{Ref}}(\lambda) S_{\text{R}}(\lambda) \mathrm{d}\lambda \int_{\lambda_1}^{\lambda_2} E_{\text{S}}(\lambda) S_{\text{T}}(\lambda) \mathrm{d}\lambda}{\int_{\lambda_1}^{\lambda_2} E_{\text{Ref}}(\lambda) S_{\text{T}}(\lambda) \mathrm{d}\lambda \int_{\lambda_1}^{\lambda_2} E_{\text{S}}(\lambda) S_{\text{R}}(\lambda) \mathrm{d}\lambda}, \tag{2}$$

where E_{Ref} is the reference spectral irradiance, E_{S} is the source spectral irradiance, S_{R} is the spectral responsivity of the reference cell, and S_{T} is the spectral responsivity of the test cell, each as a function of wavelength (λ). The limits of integration λ_1 and λ_2 in the above equation should encompass the range of the reference cell and the test device spectral responses, and the simulator and reference spectra should encompass □1 and □2 to avoid error.[36] A matched photovoltaic reference cell is typically used as the reference detector and a solar simulator is used as the light source to minimize the deviation of M from unity. Only the normalized values and not the absolute of E_{S}, S_{R}, and S_{T} need be measured for Eq. 2. Eq. 2 is valid for any thermal or photovoltaic detector or light source provided none of the integrals are zero. In the extreme case of a laser as the light source and a thermal detector with a wavelength independent responsivity, the uncertainty in M is dominated by the uncertainty in the spectral responsivity.

The total effective irradiance of the light source (E_{eff}) can be determined from the short-circuit current of the reference cell under the source spectrum ($I^{\text{R,S}}$) from the equation

$$E_{\text{eff}} = \frac{I^{\text{R,S}} M}{CN}, \tag{3}$$

where CN is the calibration number (in units of AW^{-1}m^2) for the instrument used to measure the incident irradiance. The short-circuit current of a test cell ($I^{\text{T,R}}$) at the reference total irradiance (E_{Ref}) is given as[27, 34]

$$I^{\text{T,R}} = \frac{I^{\text{T,S}} E_{\text{Ref}} CN}{I^{\text{R,S}} M}, \tag{4}$$

where $I^{\text{T,S}}$ is the short-circuit current of a test cell measured under the source spectrum. If the simulator is adjusted so that E_{eff} it equal to E_{Ref}, then

$$I^{\text{T,R}} = \frac{I^{\text{R,R}} I^{\text{T,S}}}{I^{\text{R,S}} M}, \tag{5}$$

where $I^{\text{R,R}}$ is the calibrated short-circuit current of the reference cell under the reference spectrum and total irradiance.

2.1 SPECTRAL RESPONSIBILITY MEASUREMENTS

The calibration procedure described in the above section requires the knowledge of *M* for a given light source and a given test cell / reference cell combination. This, in turn, requires the spectral irradiance of the light source and the spectral responsivities of the test and reference cells. The spectral responsivity, $S(\lambda)$, is calculated from quantum efficiency, $QE(\lambda)$, by

$$S(\lambda) = \frac{q\lambda}{hc} QE(\lambda), \tag{6}$$

where the constant term q/hc equals 8.0655×10^5 for wavelength in units of meter and $S(\lambda)$ in units of A/W. The term $QE(\lambda)$ is basically the number of electron-hole pairs generated per incident photon in the device, multiplied by 100. To calculate the spectral mismatch factor M for various test cell/reference cell combinations, we selected four test

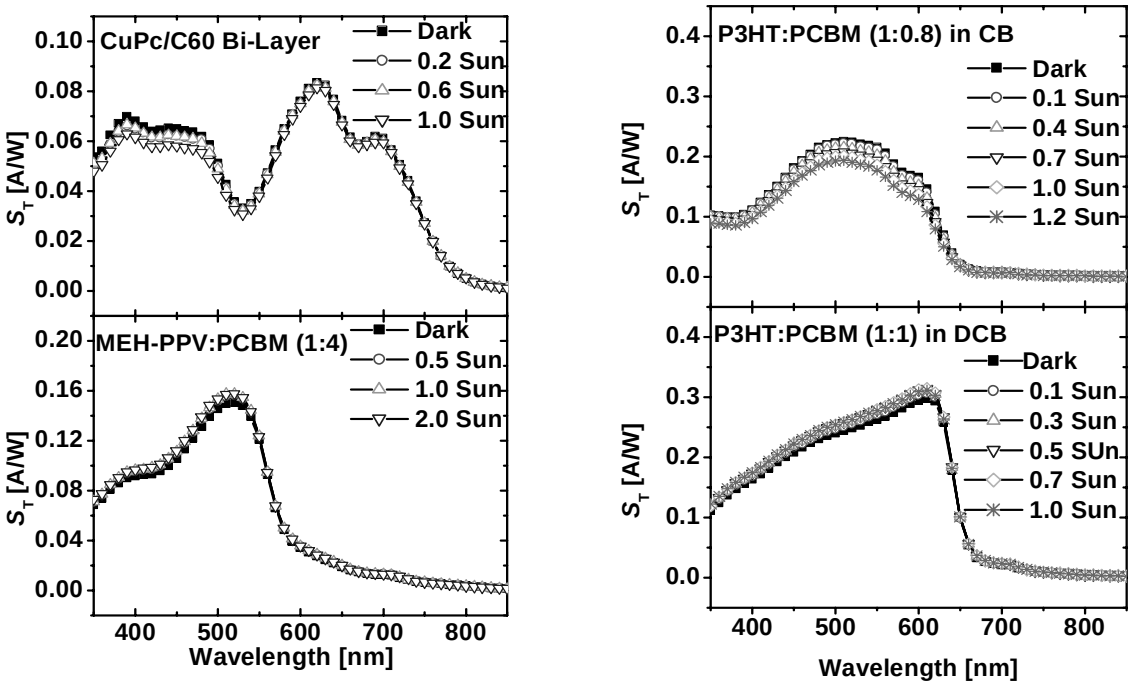

Figure 1. Spectral responsivity, $S_T(\lambda)$, under varying light-bias intensities for test cells with the following active layers: (a) CuPc/C60/BCP, (b) MEH-PPV:PCBM, (c) P3HT:PCBM(CB), and (d) P3HT:PCBM(DCB).

cells and two reference cells. The reference cells were a monocrystalline silicon diode (Newport 818-SL) and Schott color glass filtered (KG-5 color filtered) Si-diode (Hamamatsu S1133). As described in the experimental section, the typical four different types of test cells had the following active layers: (i) MEH-PPV:PCBM; (ii) P3HT:PCBM(DCB); (iii) P3HT:PCBM(CB); and (iv) CuPc/C_{60}/BCP. The spectral responsivities were measured at NREL for all the test and reference cells as per ASTM Standard E1021.The spectral responsivity measurements are typically performed at the short-circuit condition (i.e., at zero applied bias), and the relative responsivity is assumed to be the same at maximum-power and short-circuit points. The spectral responsivities of the test cells are plotted vs. wavelength in Figures 1 (a)-(d) under different light-bias intensities. The responsivities of all the cells show slight dependence on light-bias intensity, although the behavior is different for different materials systems. For CuPc/C60/BCP and P3HT:PCBM(CB), the responsivities show a small decrease when the light-bias intensity is increased from 0 to about 1 sun. On the other hand, the responsivities show a small increase for MEHPPV:PCBM and P3HT:PCBM(DCB)-based cells with increasing light-bias intensity. However, the light-bias dependence of the responsivity for all the test cells is constant with respect to wavelength, which suggests that the mismatch-factor calculation will be independent of light-bias intensity.

An important factor that has to be considered when measuring the spectral response of the PV device is the response time of the cell to the chopped light. For polymer solar cells, the response of the device to the incident light is very fast, with the response time is less than a millisecond in P3HT:PCBM(DCB) device. As a result, all the cells responded well with chopping frequencies over 150 Hz.

2.2 LIGHT SOURCE CALIBRATION AND SPECTRAL MISMATCH FACTOR

As seen from the definition of spectral mismatch, the relative spectral responsivities of the test and reference cells are important. Typically, for crystalline solar cells, the reference cell is made of the same materials and technology as the test device, which results in *M* being closer to unity. Of primary importance in a reference cell is the stability in the reference cells calibration value. For this reason most thin-film organic and inorganic devices use a Si reference cell that may have a filter to improve the spectral match. However, for polymer and organic solar cells, it is extremely difficult to fabricate reference cells from the same materials. Therefore, for the purpose of light-source calibration for organic solar cell testing, it is important to select a reference cell whose spectral response matches that of the actual test cells as closely as possible to minimize the spectral error which is not being numerically corrected for. The spectral responsivities of the two reference cells we selected are shown in Figure 2(a). Also shown is the spectral response of a thermal detector for comparison, with quantum efficiency of unity. The response of a thermal detector is very different from that of a photovoltaic cell. The unfiltered Si diode shows significant response in the wavelength range of 400-1100 nm. However, the response for Si diode with KG5 color filter is exhibited in a wavelength range of 350-700 nm. Clearly, the responsivity of the latter is similar to the responsivity of our test cells, making it more suitable for use in calibrating the light intensity of the solar simulator. This argument is further supported by calculating the mismatch factor for the four different test cells, using both the reference cells. For the purpose of calculating *M* under AM 1.5 G standard conditions, the reference spectrum used is the AM 1.5 G standard spectrum (IEC 60904) and the source irradiance spectrum is the typical irradiance spectrum for the Oriel 150 W solar simulator with AM 1.5 G filter (obtained from Newport Corporation). The reference and the source spectra used for calculating *M* are shown in Figure 2(b). The *M* values calculated by using the spectral responsivity data for different test cell / reference cell combinations are summarized in Table 1. Using a Si diode with KG5 color filter as a reference cell for light-source calibration clearly has an advantage over an unfiltered Si diode. The mismatch-factor values are very close to unity for all test cell / KG5 filtered Si-diode combinations, whereas the mismatch is between 31% and 35 % for all test cell / unfiltered Si-diode combinations. This suggests that when an unfiltered Si diode is used for calibrating the light-source intensity, possible errors due to spectral mismatch can be as high as 35%. Once M is known for a specific test cell / reference cell combination under the source spectrum, the short-circuit current of the test device under the reference spectrum can be calculated from Eqs. (4) or (5). In organic solar cells that are not limited by space-charge, such as the ones we have demonstrated here, a linear dependence of short-circuit current density (J_{SC}) with incident light intensity (I) is observed.[40] On the other hand, open-circuit voltage (V_{OC}) and fill factor (FF) depend much more weakly on I.As a result, the power conversion efficiency of organic solar cells remains almost constant in the range of 0.5 to 1 sun. A mismatch factor can therefore be used to correct the efficiency values with minimal error.

3. DEVICE AREA

To accurately determine the current density through the device, it is essential to correctly measure the device area (the total frontal area of the cell including the area covered by the grids and contacts). An important factor that can result in significant errors in the OPV cellarea estimate is the shadow effect arising from evaporating successive layers from multiple sources. One such example is the Ca/Al top electrode used in our study for all three polymer BHJ solar cells. Figure 3 shows the optical microscope image of copper (30 nm) and Au (40 nm) metal layers successively evaporated onto an ITO substrate. The two metals were chosen because the difference in film color makes it easier to see the shadow effect when observed under an optical microscope. For six different films prepared in this manner, the actual device area (defined by the overlapped area of Cu and Au films) was 91±3% of the total area. It is clear that the shadow effect can therefore result in up to 14% error in current density values. The shadow effect can be reduced significantly by adjusting the mask orientation in such a way that the device (finger) length direction is parallel to the connecting line between the sources. The device area for each device should be measured separately to correct the values of current density.

Another factor need to be taken into consideration is the lateral conductivity of interfacial layer, with the most prominent example being the high conductivity PEDOT:PSS. Figure 4a shows the configuration of the substrate with five fingers, each represent one device. We use the electronic glue to cover half of the glass substrate and use it as anode. The rest device procedure follows our former Nature Materials paper. Figure 4b shows the J-V curves of

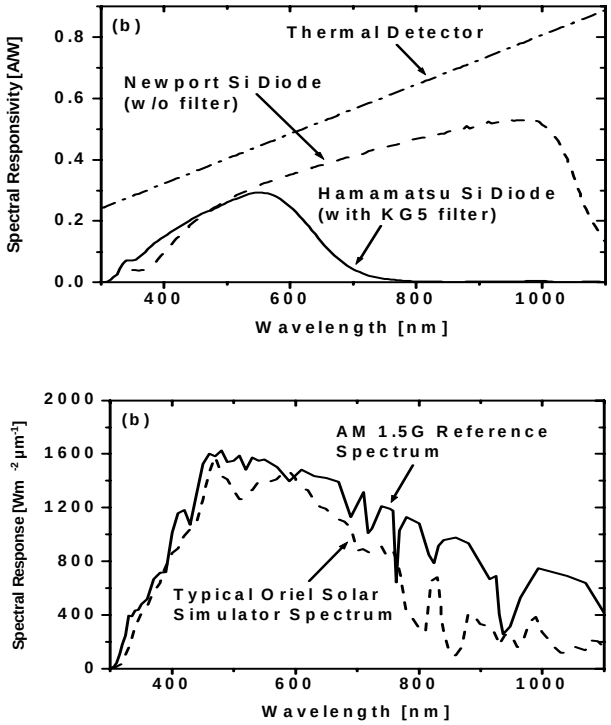

Figure 2. (a) Spectral responsivities of two types of reference cells: an unfiltered monocrystalline Si diode and a Si diode with KG5 color filter. (b) Spectral irradiance data for AM 1.5 G reference spectrum (IEC 60904)[35] and the typical source irradiance for Oriel 150 W solar simulator with AM 1.5 G filters (obtained from Newport Corporation).

Test Cell Type	Mismatch Factor	
	Si diode with KG5 color filter	Unfiltered Si diode
MEHPPV:PCBM	0.99	1.32
P3HT:PCBM(DCB)	1.01	1.35
P3HT:PCBM(CB)	1.01	1.35
CuPc/C60/BCP	0.98	1.31

Table 1. Spectral mismatch factors calculated with respect to the AM 1.5 G reference spectrum (IEC 60904) for various test cell / reference cell combinations. The spectral responsivities of the test cells used for the data shown here were measured under light bias of ~ 1 sun. The effect of light bias intensity on spectral mismatch factor was negligible (< 0.1 %).

the first four devices. The best device has a Jsc of 8.3 mA/cm^2, Voc of 0.5V, FF of 40% and an overall efficiency of 1.8%, indicates the effectiveness of the electronic glue as anode in polymer solar cell. On the other hand, although on the same substrate, we observed significant performance reduction as the distance of the device to the common anode increases. This can be easily attributed to the significantly larger resistivity of electronic glue comparing to ITO electrode.

We then compared two types of devices on ITO covered glass substrate. One with low conductivity PEDOT:PSS (Baytron P V Al 4083) and the other with electronic glue, both covers the whole substrate. As shown in Figure 5a, the most significant difference is the photocurrent, with the low conductivity PEDOT:PSS device has Jsc of 9.4 mA/cm^2 and efficiency of 3.8%, the one with electronic glue shows a descent 14 mA/cm^2 Jsc and power conversion efficiency of 5.2%. Although looks very exciting, the high efficiency is not real, because it uses the same active area (overlap of metal electrode and ITO) as the one with low conductivity PEDOT:PSS, where the lateral conductivity effect can be ignored. The JV is a combination of two subcells – one with ITO/e-glue/polymer blend/metal and one

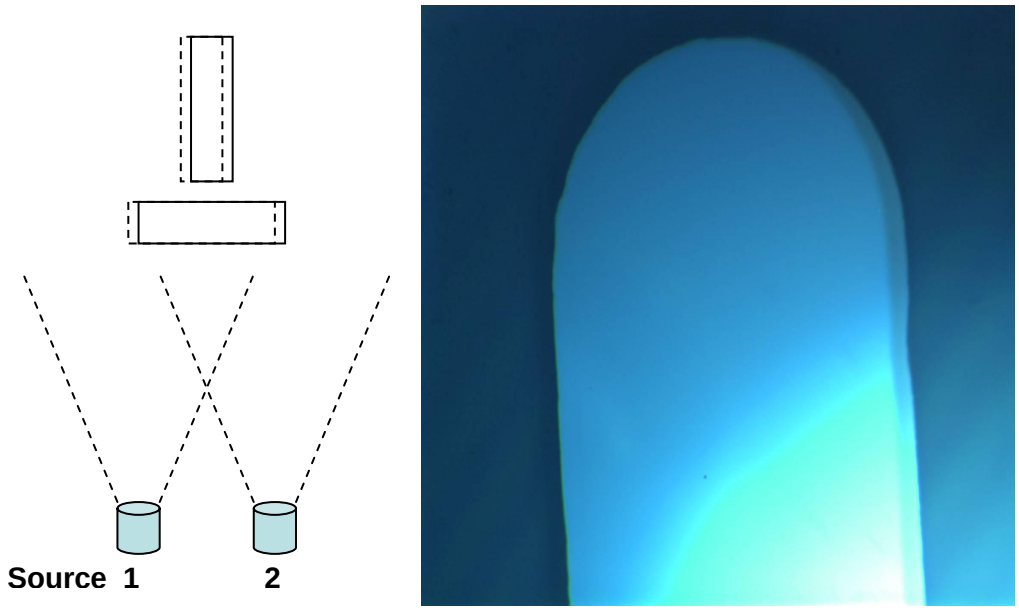

Figure 3. The optical microscope image of Cu and Au layers evaporated on an ITO substrate to demonstrate the shadow effect. A diagram is is used to illustrate the effect.

with e-glue/polymer blend/metal, and thus the significant enhancement in photocurrent can be understand. To get the correct efficiency of OPV with electronic glue as buffer layer between ITO and active layer, we use type to cover the glass only area before application of the electronic glue. The area real device area is thus the same as the device with low conductivity PEDOT:PSS cover the whole substrate. The achieved Jsc is 8.7 mA/cm^2, with high fill factor of 71% and total efficiency of 3.44%.

4. CONCLUSION

We have presented the methods for accurately rating the performance of organic solar cells. We discussed some of the important issues with respect to these devices, such as spectral responsivity and its behavior with light-bias intensity, incident-light intensity dependence of device parameters, and calculation and application of spectral mismatch factor for efficiency correction. Four different types of test cells and two reference cells were selected for calculating mismatch factors with respect to the AM 1.5 G reference spectrum. These typical spectral mismatch factors provide guidance in estimating spectral mismatch in different solar cell testing settings. The determination of correct device area is also discussed with examples.

ACKNOWLEDGEMENT

We thank Dr. Keith Emery and Tom Moriarty in NREL for important measurement of OPV samples and strong support on the mismatch factor determination.

EXPERIMENTAL

Both polymer/fullerene BHJ and small molecules-based bilayer solar cells were fabricated. The polymer photovoltaic (PV) devices were fabricated by spin-coating a blend of polymer:fullerene sandwiched between a transparent anode and a cathode. The anode consisted of glass substrates pre-coated with indium tin oxide (ITO), modified by spin-coating a polyethylenedioxythiophene:polystyrenesulfonate (PEDOT:PSS) layer, and the cathode consisted of Ca (~25 nm) capped with Al (~80 nm). Before device fabrication, the ITO (~150 nm)-coated glass substrates were cleaned by ultrasonic treatment in detergent, deionized water, acetone, and isopropyl alcohol sequentially. A thin layer (~ 25 nm) of PEDOT:PSS (Baytron P VP A1 4083) was spin-coated to modify the ITO surface. After baking at 120^{o}C for 1 hour, the substrates were transferred inside a nitrogen-filled glove box (< 0.1 ppm O_2 and H_2O). P3HT (regioregularity 98.5 %, MW ~ 30000, purchased from Rieke Metals, Inc. [34]; used as received) and MEH-PPV (purchased from Organic Vision, Inc.; used as received) were blended with PCBM

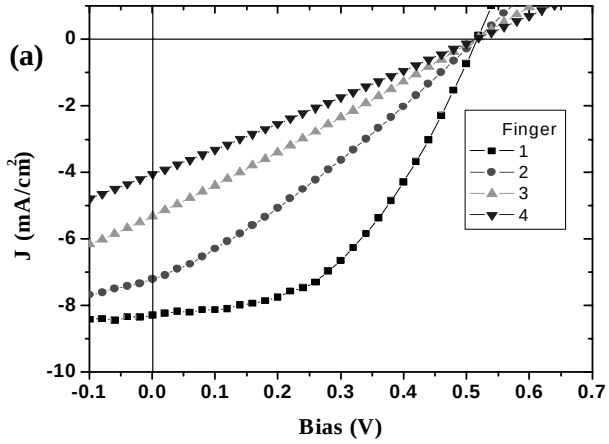

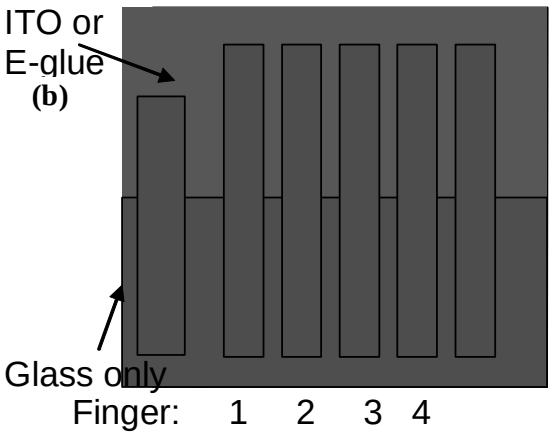

Figure 4. (a) The *I-V* characteristics for four test cells with the structure of E-glue/P3HT:PCBM/Ca/Al under 100 mW/cm^2 AM 1.5 G standard spectrum; (b) the configuration of the devices on the glass substrate.

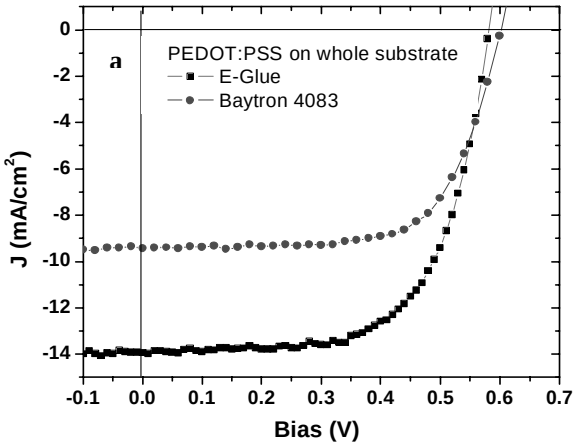

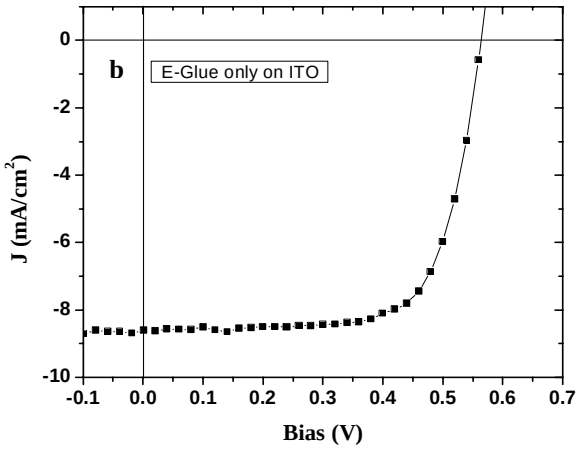

Figure 5. (a). The *I-V* characteristics for two test cells with the structure of ITO/PEDOT:PSS (E-glue vs. Baytron 4083)/P3HT:PCBM/Ca/Al under 100 mW/cm^2 AM 1.5 G standard spectrum. The PEDOT:PSS covers the whole substrate; (b) The *I-V* characteristics of the cell with the structure of ITO/ E-glue /P3HT:PCBM/Ca/Al, with the high conductivity E-glue covers only the ITO part of the substrate.

(purchased from Nano-C, Inc.; used as received) to obtain the active layer. Two different P3HT:PCBM blend solutions were prepared—1:1 wt. ratio (20 mg/ml P3HT) in 1,2-dichlorobenzene (DCB) and 1:0.8 wt. ratio (10 mg/ml P3HT) in chlorobenzene (CB)—to fabricate two types of devices named P3HT:PCBM(DCB) and P3HT:PCBM(CB), respectively. P3HT:PCBM(DCB) devices were fabricated following UCLA and UCSB approaches. The films are coated at 700 rpm (60 sec) for P3HT:PCBM(CB) devices, and then were annealed at 150ºC for 30 minutes after metal electrode evaporation. For MEH-PPV:PCBM devices, a solution of 1:4 wt. ratio (4 mg/ml MEH-PPV) in DCB was used to spin-cast the active layer. For small molecule-based devices, CuPc was selected as the active layer. The devices were fabricated by thermally evaporating successive layers of CuPc (20 nm), C_{60} (30 nm), bathocuproine (BCP) (10 nm), and Al (100 nm) onto the ITO/PEDOT:PSS substrates under a vacuum of 10^{-6} torr. The data used for spectral mismatch factor calculation are from NREL, where the encapsulated devices were shipped to NREL to test current-voltage characteristics and measure external quantum efficiency.

The high conductivity PEDOT:PSS recipe follows that of Ouyang et al's work on electronic glue, in which D-Sobitol was used to add into PEDOT:PSS. The conversion into high conductivity electronic glue was done by annealing at 110^{o}C for 10 min.

REFERENCES

[1]. C.J. Brabec, N.S. Sariciftci, and J.C. Hummelen, *Adv. Funct. Mater.* **11**, 15-26 (2001).
[2]. P. Peumans, A. Yakimov, and S.R. Forrest, *J. Appl. Phys.* **93**, 3693 (2003).
[3]. C.J. Brabec, V. Dyakonov, J. Parisi, and N.S. Sariciftci, in *Organic Photovotlaics: Concepts and Realization*, Springer (2003).
[4]. K.M. Coakley and M.D. McGehee, *Chem. Mater.* **16**, 4533-4542 (2004).
[5]. C.J. Brabec, *Solar Energy Mater. & Solar Cells* **83**, 273-292 (2004).
[6]. S.S. Sun and N.S. Sariciftci, in *Organic Photovoltaics: Mechanisms, Materials and Devices*, CRC (2005).
[7]. L.J. Lutsen, P. Adriaensens, H. Becker, A.J. Van Breemen, D. Vanderzande, and J. Gelan, *Macromolecules* **32**, 6517 (1999).
[8]. S.E. Shaheen, C.J. Brabec, F. Padinger, T. Fromherz, J.C. Hummelen, and N.S. Sariciftci, *Appl. Phys. Lett.* **78**, 841 (2001).
[9]. M.M. Wienk, J.M. Kroon, W.J.H. Verhees, J. Knol, J.C. Hummelen, P.A. van Hal, and R.A.J. Janssen, *Angew. Chem. Int. Ed.* **42**, 3371 (2003).
[10]. T. Chen and R. D. Rieke, *J. Am. Chem. Soc.* **114**, 10087 (1992).
[11]. R.D. McCullough, R.D. Lowe, M. Jayaraman, and D.L. Anderson, *J. Org. Chem.* **58**, 904 (1993).
[12]. F. Padinger, R.S. Rittberger, and N.S. Sariciftci, *Adv. Funct. Mater.* **13**, 85 (2003).
[13]. D. Chirvase, J. Parisi, J.C. Hummelen, and V. Dyakonov, *Nanotechnology* **15**, 1317 (2004).
[14]. G. Li, V. Shrotriya, Y. Yao and Y. Yang, *J. Appl. Phys.* **98**, 043704 (2005).
[15]. G. Li, V. Shrotriya, J. Huang, Y. Yao, T. Moriarty, K. Emery, and Y. Yang, *Nat. Mater.* **4**, 864 (2005).
[16]. N.S. Sariciftci, D. Braun, C. Zhang, V.I. Sradnov, A.J. Heeger, G. Stucky, and F. Wudl, *Appl. Phys. Lett.* **62**, 585 (1993).
[17]. S. Alem, R. de Bettignies, J.-M. Nunzi, and M. Cariou, *Appl. Phys. Lett.* **84**, 2178 (2004).
[18]. J.C. Hummelen, B.W. Knight, F. LePeq, F. Wudl, J. Yao, and C.L. Wilkins, *J. Org. Chem.* **60**, 532 (1995).
[19]. P. Peumans, S. Uchida, and S.R. Forrest, *Nature* **425**, 158-162 (2003).
[20]. J. Xue, S. Uchida, B.P. Rand, and S.R. Forrest, *Appl. Phys. Lett.* **85**, 5757 (2004).
[21]. F. Yang, M. Shtein, and S.R. Forrest, *Nature Materials* **4**, 37-41 (2005).
[22]. J. Drechsel, B. Männig, F. Kozlowski, D. Gebeyehu, A. Werner, M. Koch, K. Leo, and M. Pfeiffer, *Thin Solid Films* **451**, 515 (2004).
[23]. J. Drechsel, B. Männig, D. Gebeyehu, M. Pfeiffer, K. Leo, and H. Hoppe, *Org. Electron.* **5**, 175 (2004).
[24]. C.-W. Chu, Y. Shao, V. Shrotriya, and Y. Yang, *Appl. Phys. Lett.* **86**, 243506 (2005).
[25]. S. Yoo, B. Domercq, and B. Kippelen, *Appl. Phys. Lett.* **85**, 5427 (2004).
[26]. K. Emery and C. Osterwald, *Sol. Cells* **17**, 253 (1986).
[27]. K. Emery and C. Osterwald, *Current Topics in Photovoltaics*, Vol. 3, Chap. 4, Academic Press, London 1988.
[28]. K. Emery, in *Handbook of Photovoltaic Science and Engineering* (Ed: A. Luque and S. Hegedus), Chap. 16, John Wiley & Sons, Ltd., W. Sussex, 2003.
[29]. J. Rostalski and D. Meissner, *Sol. Energy Mater. Sol. Cells* **61**, 87 (95).
[30]. J.M. Kroon, M.M. Wienk, W.J.H. Verhees, and J.C. Hummelen, *Thin Solid Films* **403-404**, 223 (2002).
[31]. Standard IEC 60904-3, Measurement Principles for Terrestrial PV Solar Devices with Reference Spectral Irradiance Data, International Electrotechnical Commission, Geneva, Switzerland.
[32]. Standard IEC 60904-1, Photovoltaic devices Part 1: Measurement of Photovoltaic Current-voltage Characteristics, International Electrotechnical Commission, Geneva, Switzerland.

[33]. ASTM Standard G159, Standard Tables for Reference Solar Spectral Irradiances: Direct Normal and Hemispherical on 37° Tilted Surface, American Society for Testing and Materials, West Conshocken, PA
[34]. ASTM Standard G173, Standard Tables for Reference Solar Spectral Irradiances: Direct Normal and Hemispherical on 37° Tilted Surface, American Society for Testing and Materials, West Conshocken, PA,
[35]. Standard ASTM E948, Standard Test Method for Electrical Performance of Non-Concentrator Photovoltaic Cells Using Reference Cells, American Society for Testing and Materials, West Conshocken, PA, USA.
[36]. H. Field and K. Emery, Proc. 23rd IEEE Photovoltaic Specialist Conf., 1180 (1993).
[37]. Standard ASTM E1021, Standard Test Methods for Measuring Spectral Response of Photovoltaic Cells, American Society for Testing and Materials, West Conshocken, PA, USA.
[38]. K. Emery, D. Dunlavy, H. Field, and T. Moriarty, Proc. 2nd World Conf. and Exhibition on Photovoltaic Solar Energy Conversion, 2298 (1998).
[39]. P.M. Sommeling, H.C. Rieffe, J.A.M. van Roosmalen, A. Schönecker, J.M. Kroon, J.A. Wienke, and A. Hinsch, *Sol. Energy Mater. Sol. Cells* **62**, 399 (2000).
[40]. L.J.A. Koster, V.D. Mihailetchi, R. Ramaker, and P.W.M. Blom, *Appl. Phys. Lett.* **86**, 123509 (2005).